

# Electromagnetic reactions of few-body systems with the Lorentz integral transform method

W. Leidemann

*Department of Physics, George Washington University, Washington DC 20053, USA  
and Istituto Nazionale di Fisica Nucleare, Gruppo Collegato di Trento, Italy\**

## Abstract

Various electromagnetic few-body break-up reactions into the many-body continuum are calculated microscopically with the Lorentz integral transform (LIT) method. For three- and four-body nuclei the nuclear Hamiltonian includes two- and three-nucleon forces, while semirealistic interactions are used in case of six- and seven-body systems. Comparisons with experimental data are discussed. In addition various interesting aspects of the  $^4\text{He}$  photodisintegration are studied: investigation of a tetrahedral symmetry of  $^4\text{He}$  and a test of non-local nuclear force models via the induced two-body currents.

arXiv:nucl-th/0701034v1 12 Jan 2007

---

\*On leave of absence from Dipartimento di Fisica, Università di Trento, I-38050 Povo (Trento), Italy

## I. THE LORENTZ INTEGRAL TRANSFORM METHOD

The LIT method was introduced about a decade ago [1]. It makes feasible calculations of observables, where many-body continuum states are involved. In the LIT approach explicit calculations of continuum state wave functions are avoided, but nonetheless the continuum state interaction is fully taken into account. This is achieved via the use of integral transforms with a formal reduction of an A-body continuum state problem to an A-body bound-state-like problem [2] much simpler to solve. The method can be applied to inclusive and exclusive reactions; here we will only describe the inclusive case briefly.

Inclusive observables are expressed in terms of response functions

$$R(\omega) = \sum_f |\langle f|\hat{O}|0\rangle|^2 \delta(\omega - E_f + E_0), \quad (1)$$

where  $|0/f\rangle$  and  $E_{0/f}$  are wave functions and energies of ground and final states, respectively, while the transition operator  $\hat{O}$  defines the specific  $R(\omega)$ . The first step in a LIT calculation consists in the solution of the equation

$$(H - E_0 - \sigma_R + i\sigma_I)|\tilde{\Psi}\rangle = \hat{O}|0\rangle, \quad (2)$$

where  $H$  is the nuclear Hamiltonian and  $\sigma_{R/I}$  denote free real parameters. Due to the asymptotically vanishing ground state on the right-hand side and the complex energy term on the left-hand side,  $\tilde{\Psi}$  is localized and thus eq. (2) can be solved with bound-state methods. In a next step one determines the norm  $\langle\tilde{\Psi}|\tilde{\Psi}\rangle$ . Using closure one can show [1] that it is related to an integral transform of  $R(\omega)$  with a Lorentzian kernel, i.e. the LIT:

$$\langle\tilde{\Psi}|\tilde{\Psi}\rangle = \int d\omega \frac{R(\omega)}{(\omega - \sigma_R)^2 + \sigma_I^2}. \quad (3)$$

Calculating the LIT for many values of  $\sigma_R$  and fixed  $\sigma_I$  enables one to invert the transform reliably in order to obtain  $R(\omega)$  (for inversion methods see [3]). For the solution of  $\tilde{\Psi}$  we use expansions in hyperspherical harmonics (HH). To improve the convergence of the expansion we use two different methods: (i) CHH expansions with additional two-body correlation functions [4] and (ii) EIH expansion with an HH effective interaction [5].

## II. RESULTS AND DISCUSSION

In the following we discuss various inclusive reactions for nuclei with up to 7 nucleons:  ${}^3\text{H}/{}^3\text{He}$  ( $e, e'$ ) longitudinal form factors  $R_L(\omega, q)$  (CHH calculations with realistic nuclear

forces [6, 7]) and total photoabsorption cross sections  $\sigma_\gamma(\omega)$  of 4-, 6- and 7-body nuclei (EIHH calculations with realistic nuclear force for  $A=4$  [8] and semirealistic NN potentials for  $A=6, 7$  [9, 10]). In case of  $R_L$  we take the non-relativistic (n.r.) nuclear charge operator as transition operator  $\hat{O}$ , but also include relativistic corrections (Darwin-Foldy and spin-orbit terms). For the calculation of  $\sigma_\gamma$  we use the unretarded dipole approximation, which is excellent for  $\omega < 50$  MeV as was shown in two- and three-nucleon studies.

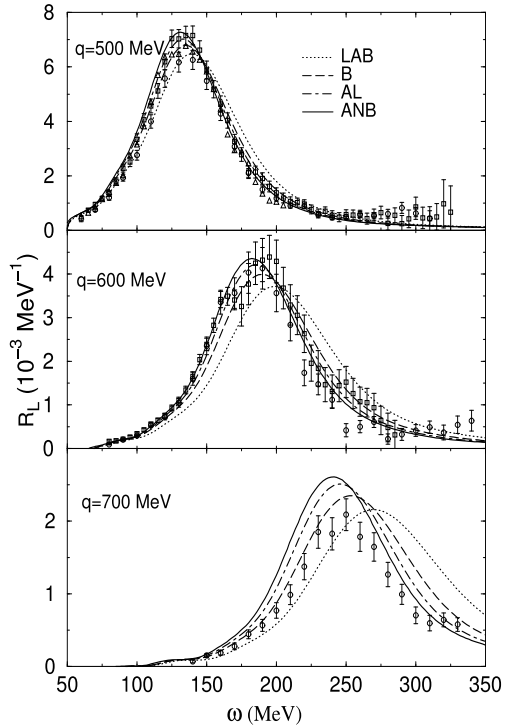


FIG. 1:  $R_L(\omega, q)$  of  ${}^3\text{He}$  at various  $q$  calculated in different frames (see text); experimental data from [11] (triangles), [12] (squares), [13] (circles).

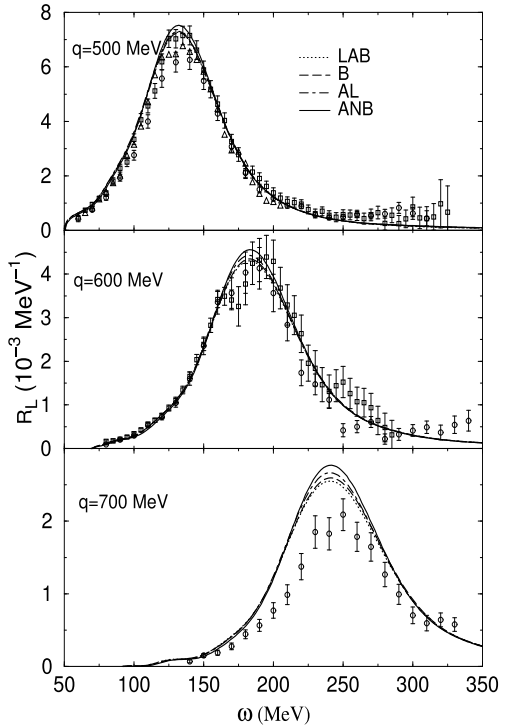


FIG. 2: As Fig. 1 but using two-body relativistic kinematics for the final state energy as discussed in the text.

In [6] we calculated  $R_L(\omega, q)$  of  ${}^3\text{H}/{}^3\text{He}$  at  $250 \text{ MeV}/c \leq q \leq 500 \text{ MeV}/c$  with the AV18 NN and the UIX 3N potentials. We found that the 3N-force reduces the quasielastic (q.e.) peak height, which improves the agreement with experimental data in case of  ${}^3\text{He}$ , but worsens the agreement in the triton case. On the other hand it should be noted that the experimental situation is more settled for  ${}^3\text{He}$ , since there one has two independent data sets and not only one as in the  ${}^3\text{H}$  case. It is interesting to study the validity of a

n.r.  $R_L$  calculation for increasing  $q$ . A kind of minimal check is made by calculating the  $R_L^{\text{fr}}(\omega_{\text{fr}}, q_{\text{fr}})$  of different reference frames and by transforming them relativistically correctly to the laboratory system (note our definition  $R_L(\omega, q) \equiv R_L^{\text{lab}}(\omega_{\text{lab}}, q_{\text{lab}})$ ) according to

$$R_L(\omega, q) = \frac{q^2}{q_{\text{fr}}^2} \frac{E_T^{\text{fr}}}{M_T} R_L^{\text{fr}}(\omega_{\text{fr}}, q_{\text{fr}}), \quad (4)$$

where  $E_T^{\text{fr}}$  and  $M_T$  are energy and mass of the target nucleus. In Fig. 1 we show results for four different frames [7], which are defined via the target nucleus initial momentum  $\mathbf{P}_T^{\text{fr}}$ :  $\mathbf{P}_T^{\text{lab}}=0$ ,  $\mathbf{P}_T^{\text{B}} = -\mathbf{q}/2$ ,  $\mathbf{P}_T^{\text{AL}} = -\mathbf{q}$ ,  $\mathbf{P}_T^{\text{ANB}} = -3\mathbf{q}/2$ . It is readily seen that one obtains more and more frame dependent results with growing  $q$ . As shown in [7] the frame dependence can be drastically reduced if one imposes q.e. kinematics and takes the relativistic relative momentum between knocked-out nucleon and residual two-body system as input in the calculation. As seen in Fig. 2 one finds almost frame independent results, which show a very good agreement with experimental data at  $q = 500$  and  $600$  MeV/c, while at  $700$  MeV/c the experimental peak height is considerably lower than the theoretical one. We would like to point out that the ANB result of Fig. 1 lies within the band of almost frame independent results of Fig. 2. Thus we consider the ANB frame as the optimal frame for a n.r. calculation. It leads to a proper description of the q.e. peak region, however, with no need to assume q.e. kinematics and thus its validity is not restricted to the peak region (further explanations why the ANB system is preferable are given in [7]).

Now we turn to nuclear photodisintegration and first discuss  $A \geq 6$  nuclei. In Fig. 3 we show  $\sigma_\gamma(\omega)$  of  ${}^6\text{He}$  and  ${}^6\text{Li}$  calculated with various semirealistic NN potential models: Malfiet-Tjon (MT), Minnesota (MN), and Argonne V4' (AV4') [9]. Particularly interesting are the  ${}^6\text{He}$  results, they show two separate peaks. In a many-body picture they correspond to a soft mode at low energies, where the surface neutrons oscillate against the  $\alpha$ -core, and a Gamov-Teller mode at higher energies, where the neutrons oscillate against the protons. It is worthwhile to point out that such a double peak structure comes out also in our microscopic few-body calculation. For a comparison with experiment we refer to [9], here we show a comparison with data for the  ${}^7\text{Li}$  case [10] (see Fig. 4). It is evident that there is a rather good agreement between theory and experiment, which also shows that with the LIT calculation one has a reliable control of the seven-body continuum.

The experimental study of the  ${}^4\text{He}$  photodisintegration has a rather long history. First experiments have been carried out about 50 years ago. Much work was devoted to the

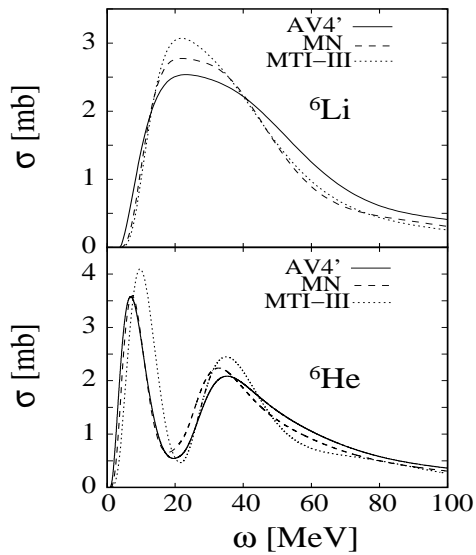


FIG. 3: Total photoabsorption cross sections of  ${}^6\text{Li}$  and  ${}^6\text{He}$  calculated with various semirealistic potential models.

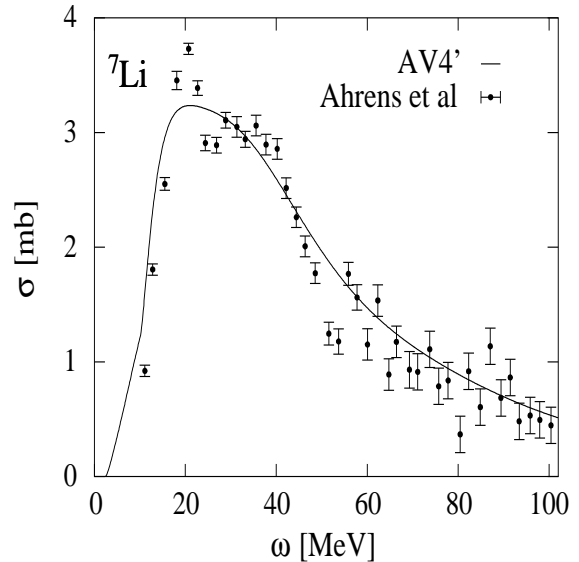


FIG. 4:  ${}^7\text{Li}$  total photoabsorption cross section calculated with the AV4' potential; experimental data from [14].

two low-energy two-body break-up channels of  ${}^3\text{H}-p$  and  ${}^3\text{He}-n$ . The results were rather controversial showing either a very pronounced giant dipole peak or a rather flat structure. In the '80s and '90s data seemed to converge to a less pronounced peak [15, 16], which, however, is at variance with a following determination via Compton scattering [17]. In one of our first LIT applications we calculated  $\sigma_\gamma(\omega)$  of  ${}^4\text{He}$  using semirealistic potential models [18]. In contrast to the experiments of [15, 16] we found a very pronounced giant dipole peak, which also revived experimental activities (see [19, 20]). A very important further theoretical clarification comes from our recent calculation of  $\sigma_\gamma({}^4\text{He})$  with a realistic nuclear force (AV18+UIX) [8]. In Fig. 5 one sees that the 3N-force leads to a reduction of the peak height, but that the full AV18+UIX result shows a pronounced peak and thus confirms the findings of [18]. In comparison to experiment one observes a rather good agreement with the data of [19] (note: measured  $(\gamma, n)$  cross section is doubled assuming that it is about equal to the  $(\gamma, p)$  cross section; only statistical errors are shown), while the data of [20] are much lower and do not exhibit any low-energy peak.

A calculation of  $\sigma_\gamma$  in unretarded dipole approximation has the great advantage that also the dominant part of the meson exchange current (MEC) contribution is considered (Siegert

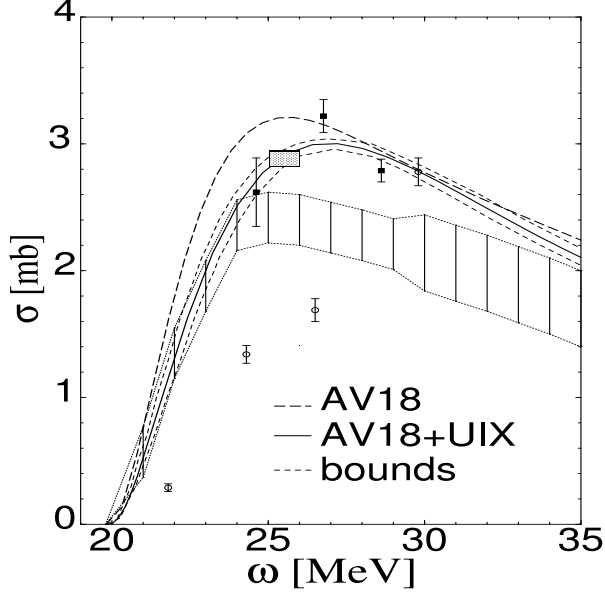


FIG. 5:  ${}^4\text{He}$  total photoabsorption cross section with AV18+UIX (with upper and lower bounds due to uncertainties of HH expansion convergence) and AV18 potentials; experimental data (see also text): area between dotted lines [15, 16], dotted box [17], squares [19], and circles [20].

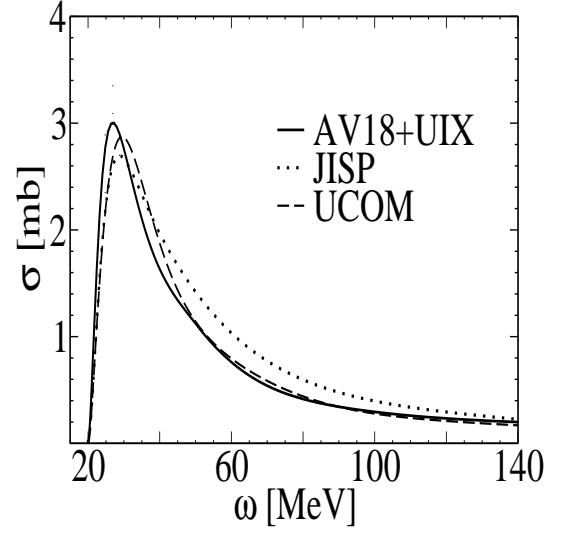


FIG. 6: As Fig. 5 but calculated with AV18+UIX, JISP and UCOM potentials.

theorem). Thus  $\sigma_\gamma$  is an ideal testground for nuclear potential models: one works with a very simple transition operator  $\hat{O}$ , but nonetheless includes an important MEC contribution. Compared to purely hadronic reactions one obtains additional valuable information about a given nuclear force model. We take advantage of this fact and test potentials [21, 22] designed for the use in more complex nuclei (JISP models [23], UCOM [24]), which on the one hand describe NN scattering data, but on the other hand also binding energies of nuclei with  $A > 2$  (see also contribution of G. Orlandini et al.). In Fig. 6 we show results for the  $\sigma_\gamma$  of  ${}^4\text{He}$  for these potentials in comparison to the AV18+UIX case. One sees that the peaks are a bit lower and also shifted somewhat towards higher energy for JISP and UCOM interactions. Beyond the peak there is a rather good agreement between UCOM and AV18+UIX results, while the JISP6 potential leads to a considerably higher cross section. Due to the lack of precise experimental data one cannot rule out any of these potential models.

Additional information on the electromagnetic structure of nuclei can be obtained from photonuclear sum rules. In [25] we have considered various  ${}^4\text{He}$  sum rules with the AV18+UIX potential, but here we only discuss the  ${}^4\text{He}$  bremsstrahlungs sum rule

$$\Sigma_{\text{BSR}} = \int_{\omega_{th}}^{\infty} d\omega \frac{\sigma_{\gamma}^{E1UR}}{\omega}, \quad (5)$$

where  $\sigma^{E1UR}$  is  $\sigma_{\gamma}$  in unretarded dipole approximation. One also has [25]

$$\frac{\Sigma_{\text{BSR}}}{g} = Z^2 \langle r_p^2 \rangle - \frac{Z(Z-1)}{2} \langle r_{pp}^2 \rangle = N^2 \langle r_n^2 \rangle - \frac{N(N-1)}{2} \langle r_{nn}^2 \rangle = \frac{NZ}{2} \left( \langle r_{np}^2 \rangle - \langle r_n^2 \rangle - \langle r_p^2 \rangle \right) \quad (6)$$

with  $g = 4\pi^2\alpha/3$  and where  $\langle r_{p/n}^2 \rangle$  is the mean square proton/neutron radius and  $\langle r_{pp/nn/np}^2 \rangle$  is the mean square distance between nucleons in a pp/nn/np-pair. Neglecting the tiny isospin breaking part of the NN interaction, for  ${}^4\text{He}$  one has  $\langle r_p^2 \rangle = \langle r_n^2 \rangle$ . In case of the AV18+UIX potential one finds  $\langle r_{n/p}^2 \rangle = 2.04 \text{ fm}^2$ , which is in agreement with the  ${}^4\text{He}$  experimental charge radius. Thus an additional determination of  $\Sigma_{\text{BSR}}$  leads to the various NN mean square distances. Our evaluation for AV18+UIX yields a  $\Sigma_{\text{BSR}}$  value of 2.410 mb leading to 5.67  $\text{fm}^2$  ( $\langle r_{pp/nn}^2 \rangle$ ) and 5.34  $\text{fm}^2$  ( $\langle r_{np}^2 \rangle$ ). The difference between the two values is caused by the isospin dependence of the nuclear force (pp/nn-pairs: isospin T=1, np-pairs: T=0,1). It is interesting to note that the ratios  $\langle r_{pp}^2 \rangle / \langle r_p^2 \rangle = 2.78$  and  $\langle r_{np}^2 \rangle / \langle r_p^2 \rangle = 2.62$  are very close to the value for a tetrahedral symmetry of 2.67 [25]. Thus one may conclude that the  ${}^4\text{He}$  two-body density reflects to a large extent such a symmetry.

It follows a short summary of this presentation. It has been shown that the LIT method is a very powerful tool: a continuum state problem is reduced to a bound-state-like problem. It enables one to make ab initio calculations of reactions with light nuclei into the many-body continuum. Among the discussed applications is the first cross section calculation of a four-body reaction into the four-body continuum ( ${}^4\text{He}$  total photoabsorption cross section) evaluated with a realistic nuclear force (AV18+UIX). The results show a pronounced giant resonance peak, while the experimental data do not lead to a unique picture and hence further experimental investigations are certainly necessary.

---

[1] V.D. Efros, W. Leidemann and G. Orlandini, Phys. Lett. B 338 (1994) 130.

[2] V.D. Efros, Yad. Fiz. 41 (1985) 498.

- [3] V.D. Efros, W. Leidemann and G. Orlandini, *Few-Body Syst.* 26 (1999) 251;  
D. Andreasi et al., *Eur. Phys. J. A* 17 (2003) 589.
- [4] V.D. Efros et al., *Phys. Lett. B* 484 (2000) 223.
- [5] N. Barnea, W. Leidemann and G. Orlandini, *Phys. Rev. C* 61 (2000) 054001.
- [6] V.D. Efros et al. *Phys. Rev. C* 69 (2004) 044001.
- [7] V.D. Efros et al., *Phys. Rev. C* 72 (2005) 011002(R).
- [8] D. Gazit et al., *Phys. Rev. Lett.* 96 (2006) 112301.
- [9] S. Bacca et al., *Phys. Rev Lett.* 89 (2002) 052502, *Phys. Rev. C* 69 (2004) 057001.
- [10] S. Bacca et al., *Phys. Lett. B* 603 (2004) 159.
- [11] C. Marchand et al., *Phys. Lett. B* 153 (1985) 29.
- [12] K. Dow et al., *Phys. Rev. Lett.* 61 (1988) 1706.
- [13] J. Carlson et al., *Phys. Rev. C* 65 (2002), 024002.
- [14] J. Ahrens et al., *Nucl. Phys. A* 251 (1975) 479.
- [15] B.L. Berman et al., *Phys. Rev. C* 22 (1980) 2273.
- [16] G. Feldman et al., *Phys. Rev. C* 42 (1990) 1167.
- [17] D.P. Wells et al., *Phys. Rev. C* 46 (1992) 449.
- [18] V.D. Efros, W. Leidemann and G. Orlandini, *Phys. Rev. Lett.* 78 (1997) 4015;  
N. Barnea et al., *Phys. Rev. C* 63 (2001) 057002.
- [19] B. Nilsson et al., *Phys. Lett. B* 626 (2005) 65.
- [20] T. Shima et al., *Phys. Rev. C* 72 (2005) 044004.
- [21] N. Barnea, W. Leidemann and G. Orlandini, *Phys. Rev. C* 74 (2006) 034003.
- [22] S. Bacca, [nucl-th/0612016](https://arxiv.org/abs/nucl-th/0612016).
- [23] A.M. Shirokov et al., *Phys. Lett. B* 621 (2005) 96.
- [24] R. Roth et al., *Nucl. Phys. A* 745 (2004) 3.
- [25] D. Gazit et al., *Phys. Rev. C* 74 (2006) 061001(R).